

Fuzzy Impedance Control Strategy for Jaw Rehabilitation Using 6-UPS Stewart Robot

Hadi Kalani

Center of Excellence on Soft Computing and Intelligent
Information Processing
Mechanical Engineering Department, Ferdowsi University
of Mashhad, Mashhad, Iran
hadi.kalani@yahoo.com

Alireza Akbarzadeh

Center of Excellence on Soft Computing and Intelligent
Information Processing
Mechanical Engineering Department, Ferdowsi University
of Mashhad, Mashhad, Iran
ali_akbarzadeh@um.ac.ir

Ali Mousavi

Center of Excellence on Soft Computing and Intelligent Information Processing
Mechanical Engineering Department, Ferdowsi University of Mashhad, Mashhad, Iran
ali_mousavi68@yahoo.com

Abstract—Recently, the variety of devices and robots are available for recovering and rehabilitating human disorder patients. In this paper, simple and effective control method utilized for position-impedance control. This method consists of two parts, namely position control in free space and fuzzy impedance control in contact. First, kinematics and dynamics of general 6UPS are discussed. Then SimMechanics software is employed to validate dynamics equations. Next an impedance filter is developed. The gains of this filter are adjusted by fuzzy logic method to achieve the reference force. In order to reproduce jaw motions and apply the impedance control, the workspace of human jaw is needed. To obtain this workspace, three male subjects (age range 24–28 years) were selected. Results show that the fuzzy impedance control is suitable to control of masticatory robots.

Keywords— *Stewart Platform Robot, Fuzzy Impedance Control, Mastication Robots, Position Control.*

I. INTRODUCTION

The human chewing process has been investigated in various studies. In general, mastication involves two simple movements: clenching and grinding. In clenching, the jaw moves only in the sagittal plane, whereas in grinding it follows a circle path in the frontal plane [1], [2]. The temporalis, masseter and lateral Pterygoid muscles perform the main role in the mastication process. Recently, EMG signals have been employed in rehabilitation applications to study changes of muscles' electrical activity during mastication [3-6]. EMG has also been utilized to distinguish the differences between chewing patterns of individuals [7-10].

Impedance control scheme is introduced by Hogan [11]. Using this method operator can assign desired mass/inertia, damping, and stiffness to the robot. The most important feature of impedance control is handling constrained and unconstrained motion [12]. In fact robot is modeled as a mass,

spring, and damper while interacting with human or environment. This type of impedance control is usually called pure impedance control [13]. External force is not controlled in this method and it is consequence of environment and robot desired stiffness. Many researchers concentrate on force tracking impedance control [13-16]. Reference [13] has applied direct and indirect adaptive control to produces desired contact force in selected direction. Reference [14] has utilized adaptive control scheme while to track a specified desired force and to compensate for uncertainties in environment location, stiffness, and robot dynamic model. A new impedance filter is developed to achieve the desired behavior between the position and force in [15]. Reference [16] has applied impedance control in a rehabilitation robot. Then force tracking is achieved with the adaptive control, subject to uncertain human limb dynamics. In this paper a force tracking impedance control is presented and applied in 6-UPS Stewart robot.

The rest of the paper is organized as follows: Section II describes the kinematics and dynamics modeling of 6-UPS Stewart robot. Then control schematic is presented in section III. Simulation results are illustrated in section IV. Finally section V provides conclusion remarks.

II. KINEMATICS AND DYNAMICS MODELLING OF STEWART PLATFORM

The Gough-Stewart platform is a type of parallel manipulator, which consists of a mobile platform and a stationary base, connected to each other by six linear actuators. Consider Fig. 1. Frame {T} and frame {B} are attached to the moving platform and fixed base, respectively.

Six closed vector-loop equations can be written as

$${}^B \mathbf{a}_i + {}^B \mathbf{q}_i^{ac} = {}^B \mathbf{R}^T \mathbf{b}_i + {}^B \mathbf{p}, \text{ for } i = 1, 2, \dots, 6 \quad (1)$$

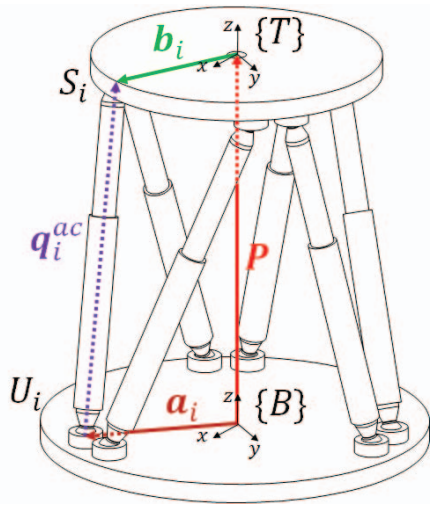


Fig. 1. A closed loop vector for i^{th} leg of the 6-UPS parallel robot

where ${}^B\mathbf{R}$ is a rotation matrix to transfer a vector defined in $\{T\}$ to $\{B\}$. Vectors ${}^B\mathbf{a}_i$, ${}^T\mathbf{b}_i$ and ${}^B\mathbf{p}$ denote position of point U_i relative to frame $\{B\}$, position of point S_i relative to frame $\{T\}$ and the translation vector of the tip, point P , respectively. The actuated joints values, ${}^B\mathbf{q}_i^{ac}$, and unit vectors along the actuated prismatic joints, ${}^B\hat{\mathbf{q}}_i^{ac}$, can be calculated using (2) as

$$q_i^{ac} = \left\| {}^B\mathbf{R}^T \mathbf{b}_i + {}^B\mathbf{p} - {}^B\mathbf{a}_i \right\|, \text{ for } i = 1, 2, \dots, 6 \quad (2)$$

$$\hat{\mathbf{q}}_i^{ac} = \frac{1}{q_i^{ac}} \left\| {}^B\mathbf{R}^T \mathbf{b}_i + {}^B\mathbf{p} - {}^B\mathbf{a}_i \right\|, \text{ for } i = 1, 2, \dots, 6 \quad (3)$$

The overall inverse velocity relation for the 6-UPS parallel robot can be obtained in familiar matrix form as

$$\mathbf{q}^{ac} = \mathbf{J}_{MP} \dot{\mathbf{X}}_a \quad (4)$$

where \mathbf{J}_{MP} is a 6×6 square matrix called inverse Jacobian matrix of the 6-UPS parallel robot and $\dot{\mathbf{X}}_r$ the twist vector of the moving platform. Clearly, to obtain the overall direct velocity relation for the 6-UPS parallel robot can be written as

$$\dot{\mathbf{X}}_r = \mathbf{J}_{MP}^{-1} \mathbf{q}^{ac} \quad (5)$$

By employing principle of virtual work the equations of motion of the robot can be expressed as [19]

$$\mathbf{M}(\mathbf{q}) \ddot{\mathbf{q}}^{ac} + \mathbf{C}(\mathbf{q}, \dot{\mathbf{q}}) \dot{\mathbf{q}}^{ac} + \mathbf{G}(\mathbf{q}) + \mathbf{w} + \mathbf{f}^{ac} = \mathbf{0}_{6 \times 1} \quad (6)$$

where $\mathbf{M}(\mathbf{q})_{6 \times 6}$ is a positive definite and symmetric inertia matrix, $\mathbf{C}(\mathbf{q}, \dot{\mathbf{q}})$ represents centrifugal and Coriolis terms, \mathbf{f}^{ac} is the actuated forces, $\mathbf{G}(\mathbf{q})$ represents the potential energy, and \mathbf{w} represents external forces and torques on moving platform. The derived theoretical equations are validated by SimMechanic software (Fig. 2).

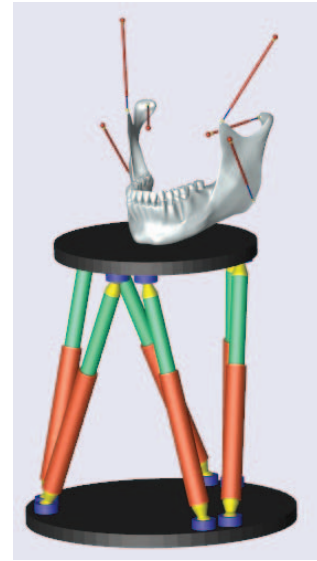


Fig. 2. Modelling of our system in SimMechanics software

It should be mentioned that more than 20 muscles are involved in the process of human mastication; only six of these muscles play a major role [6]. To represent the geometry of human mastication, we use a general 6-UPS Stewart–Gough platform. The mobile and stationary platforms represent the human jaw and skull, respectively. Therefore, as can be seen, Fig. 2 consists of two modules. One of them shows the 6-UPS to model rehabilitated robot and another one is to model mastication robot. In this study, mastication robot is developed to replicate human chewing movements and to study effect of rehabilitating trajectories in each mastication muscle.

III. CONTROL SCHEMATIC

The controller consists of three parts: PID controller, impedance filter, and fuzzy block. Fig. 3 shows a block diagram of the controller used here. Additionally, the integrator integral is added to remove the steady-state error.

A. PID Controller

Generally, position control is utilized to track a pre-defined trajectory. Proportional-Integral-Derivative (PID) is one of the most popular position controllers due to its simple structure and implementation. A large amount of position error is caused while robot collides with an obstacle through a trajectory. It may causes damage to the robot or obstacle. PID formulation is presented by (6).

$$P \times (l_r - l_a) + D \times (\dot{l}_r - \dot{l}_a) + I \times \int_0^t (l_r - l_a) dt = \tau \quad (7)$$

Where P , D , and I are proportional, derivative, and integral gains, respectively. The values of these gains are determined by trial and error. P , I , and D gains are 15000, 1000, and 200, respectively. Moreover l_a and l_r are actual and reference actuator's length.

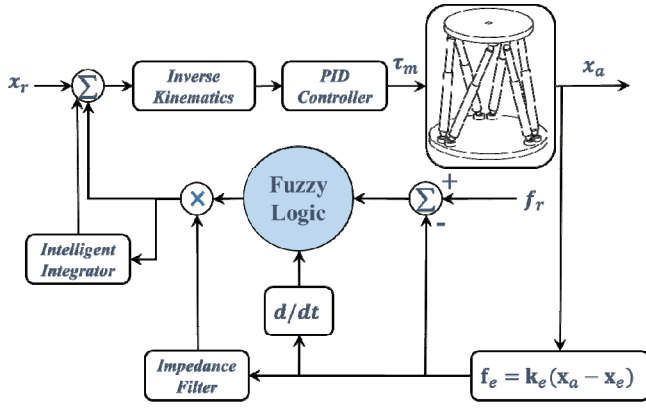


Fig. 3. Flowchart of fuzzy impedance controller

Control system block-diagram is depicted in Fig. 4-a. Position control block is illustrated in detailed as shown in Fig. 4-b.

Physical human-robot interaction needs contact force regulation in order to ensure human health. Position control is not capable of guaranteeing force regulation. This problem is more investigated in next section.

B. Impedance Filter

Impedance control scheme is an independent loop which can be added to robot position control system. In this method robot needs a force sensor installed on end-effector. Control system block-diagram is depicted in Fig. 5. The reference trajectory can be modified by result of impedance control. Equation (8) shows impedance control formula in frequency domain [17].

$$M_i s^2 + B_i s + K_i = F_{ei} \quad i = 1, 2, \dots, 6 \quad (8)$$

$$F_e = [F_{ex} \quad F_{ey} \quad F_{ez} \quad T_{ex} \quad T_{ey} \quad T_{ez}]$$

where M_i is the virtual mass, B_i is the virtual damping coefficient, K_i is the virtual spring constant, F_{ei} is the force applied to the system and i represents the 6 direction of moving platform in Cartesian space. As Fig. 5 shows reference trajectory is followed by position control unless external force is applied on the robot. When robot interacts with human or environment, external force (force and torque) is applied on force sensor. Then pre-defined trajectory can be modified by impedance control result. Interaction force is result of reference and actual end-effector position. In other words, jaw is moved using reference trajectory unless external force applied to the robot. Then impedance control modifies the reference trajectory. It should be mentioned, in this method, we are not able to achieve the reference force [13]. External force is modeled as

$$F_{ez} = K_{ez} \times (z_a - z_e) \quad (9)$$

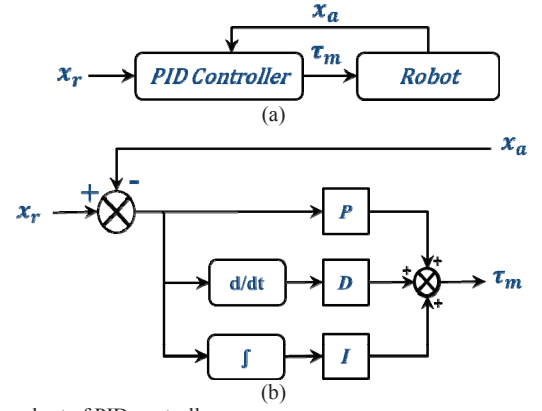


Fig. 4. Flowchart of PID controller

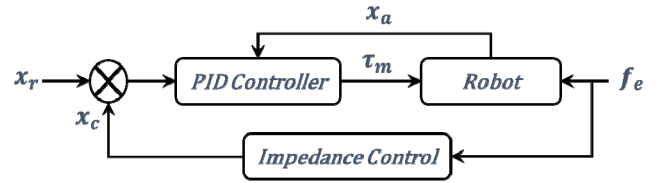


Fig. 5. Flowchart of impedance controller

where K_{ez} , z_a , and z_e represent stiffness, actual position, and allowable workspace in z-axis, respectively. In this paper, interaction is only controlled in z-axis where robot is modeled as a mass, spring, and damper (Fig. 6). Impedance parameters and k_{ez} are illustrated in table I. These values are obtained by trial and error simulation.

C. Fuzzy Controller

In this study, the goal of fuzzy logic controller is to adjust the impedance filter gain around the reference force. Additionally to remove the steady-state error, an integrator is employed in controller. In fuzzy controller, a Mamdani Max-Min, with 2 inputs (force error and rate of force) and one output (filter gain) are used. Rules and number of membership functions are selected according to trial and error simulation. In this paper, seven membership functions for each inputs and outputs are chosen. Therefore, we have 49 rules generally. These rules are summarized in table II. Moreover Fig. 7 indicates membership functions for two inputs and one output.

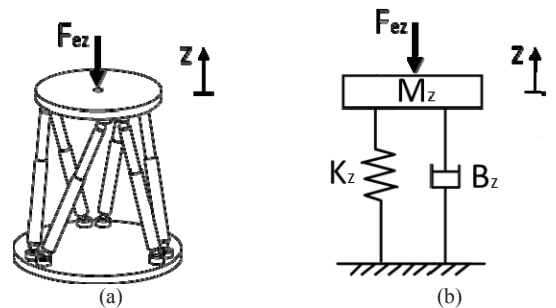


Fig. 6. (a) 6UPS platform (b) equivalent mass-spring-damper system

TABLE I. IMPEDANCE PARAMETERS

| Parameter | Value |
|-----------------------------|-------|
| M_z (N.s ² /m) | 1 |
| B_z (N.s/m) | 50 |
| K_z (N/m) | 600 |
| k_{ez} (N/m) | 1000 |

TABLE II. RULES TABLE OF FUZZY CONTROLLER

| | | Rate of force | | | | | | |
|-------------|----|---------------|----|----|----|----|----|----|
| | | nl | nm | ns | z | ps | pm | pl |
| Force Error | nl | z | ns | nm | nl | nl | nl | nl |
| | nm | z | z | ns | nm | nl | nl | nl |
| | ns | z | z | z | ns | ns | nm | nl |
| | z | pl | pm | ps | z | ns | nm | nl |
| | ps | pl | pm | ps | ps | z | z | z |
| | pm | pl | pl | pm | pm | ps | z | z |
| | pl | pl | pl | pl | pl | pm | ps | z |

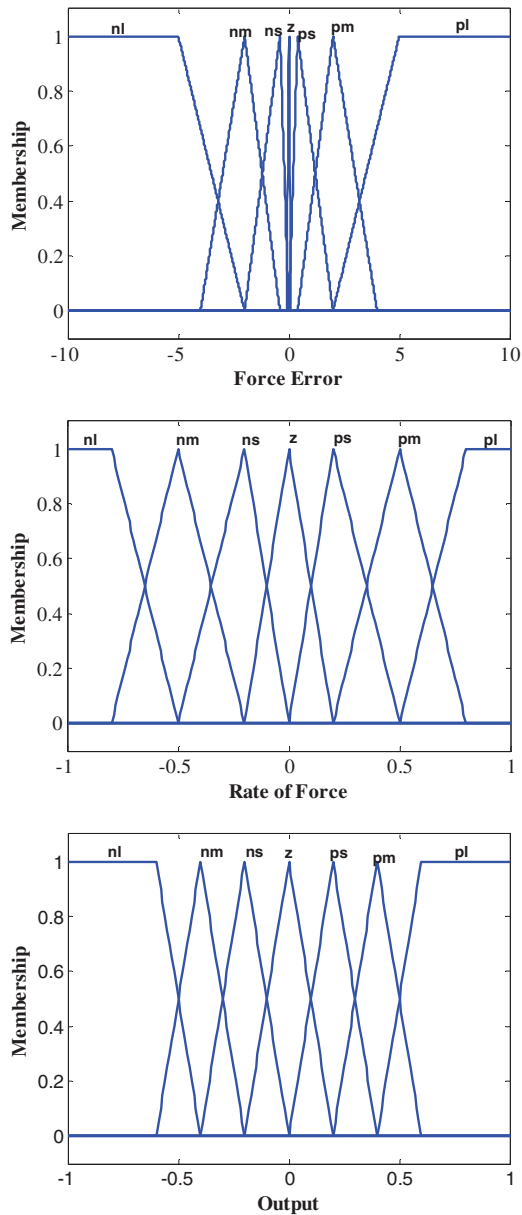


Fig. 7. Input-Output membership

IV. SIMULATION AND RESULTS

A. Recording Jaw Trajectory

To record the jaw motion, 6 small reflective markers were adhered to specific facial locations (Fig. 8). Forehead markers were used as reference points. The recorded camera signals were rectified and smoothed by a moving average window of size 200.

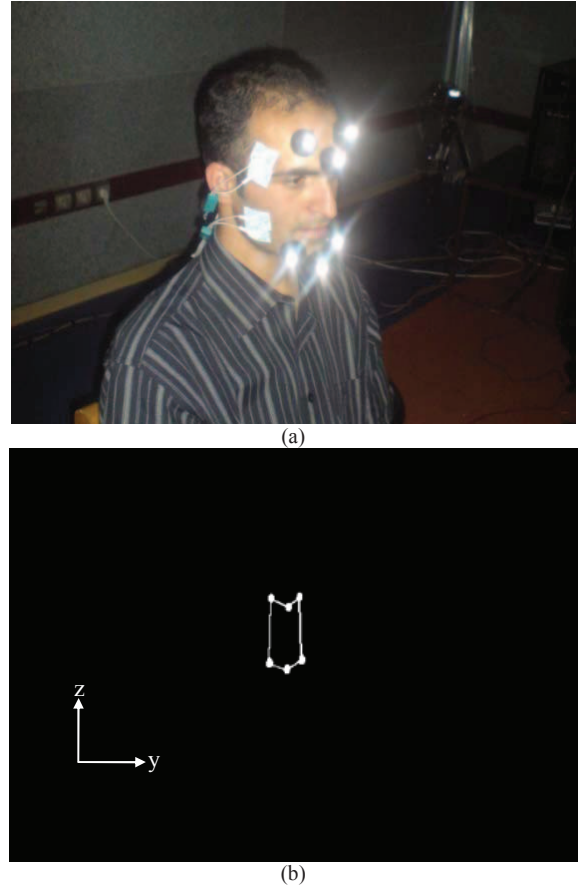


Fig. 8. (a) Marker position on the subject's face, (b) Two-dimensional reconstruction of the marker set

To obtain the chewing trajectory, three male subjects (age range 24–28 years) were selected. The recorded 3D mandibular trajectory is shown in Fig. 9. This figure shows the time-dependent trajectory of the jaw in a mastication process of subject 2.

Based on [18] and our observations, the workspace of jaw during mastication summarized in table III. These values are utilized in impedance control.

B. Control of Stewart Robot Base on Jaw Motion

This paper investigates the fuzzy impedance control of a 6-UPS platform based on a mastication trajectory. By considering this trajectory and our controller, representative postures during the trajectory are demonstrated in Fig. 10.

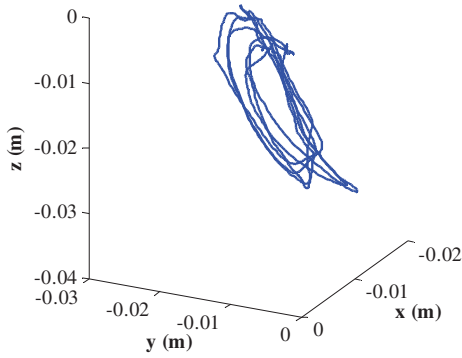


Fig. 9. Chewing trajectory, recorded from subject 2

TABLE III. WORKSPACE OF JAW MOTION

| Displacement | | | Rotation | | |
|--------------|----------|----------|-----------------|-----------------|-----------------|
| x (mm) | y (mm) | z (mm) | About x (deg) | About y (deg) | About z (deg) |
| -21 | -8 | -30 | -1 | -14 | -0.5 |
| +4 | +8 | +2 | +1 | +3 | +0.5 |

Moreover, we are able to obtain the time-varying behavior of the muscle lengths during motion (Fig 11). The temporalis muscles experienced larger length changes compared to masseter and pterygoid muscles. Also, the behavior of the muscles could be approximated by series harmonic functions.

In impedance control problem, the dynamic behavior of the robot is specified by the resultant forces in contact that are dependent on differences between the actual and reference positions of the robot. In this study impedance controller is designed as a second-order filter. Fig. 12 indicates the resultant contact force, when pure impedance control is only utilized.

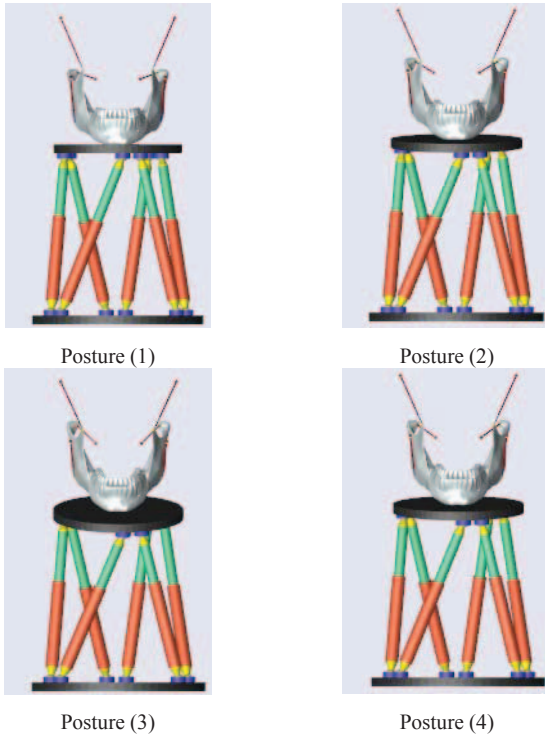


Fig. 10. Four postures of 6-UPS platform during clenching movement

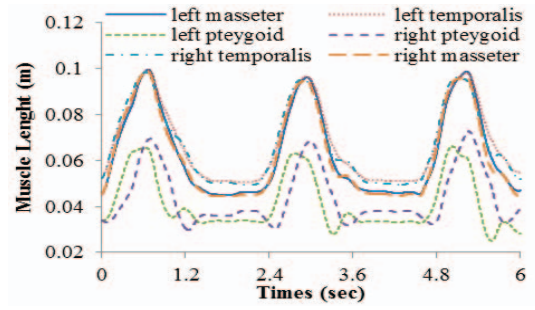


Fig. 11. Time-varying lengths of muscles during the chewing pattern.

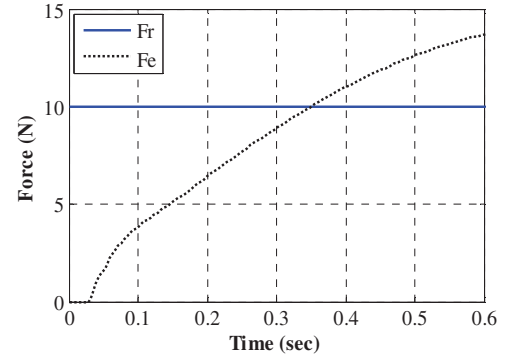


Fig. 12. Simulation responses with reference input of 10 N force along z-axis, when the pure impedance is only used.

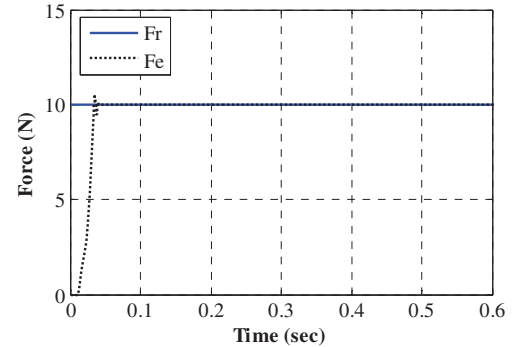


Fig. 13. Simulation responses with reference input of 10 N force along z-axis, when the impedance gains are adjusted by Fuzzy logic controller.

As can be seen in Fig. 12, we are not able to control contact force around a reference force. To eliminate this problem the fuzzy logic controller is employed to set the impedance filter gain around the reference force if the robot is in contact with any surface. Fig. 13 indicates the response force of system, when the reference force is 10 N. In another case, a 5 N force, 0.09 m position in z-axis and a sinusoidal trajectory are applied to robot as reference inputs and trajectory in the z-axis, respectively. The force response and position change of the moving platform are shown in Fig. 14. Based on Fig. 13 and Fig. 14, the fuzzy logic controller enables the robot to achieve reference force reasonably.

V. CONCLUSION

In this study impedance control is utilized to model physical interaction between robot and human jaw. Position control and pure impedance control are unable to control

contact force. In fact for safety issues, the contact force has to be saturated with a pre-defined value. Therefore impedance parameters are adjusted by a fuzzy logic controller to control contact force. Reference trajectory modified by impedance filter so that reference force is precisely followed by contact force. Simulation results show the effectiveness of the method in comparison to pure impedance control.

The analysis provided in this study will allow researchers to characterize and study the mastication process by specifying different chewing patterns and observing the resulting jaw movement. The paper contributes to the literature by using two 6-UPS architecture as rehabilitation robot and mastication robot, simultaneously and applying a fuzzy impedance controller to enable robot to achieve reference force.

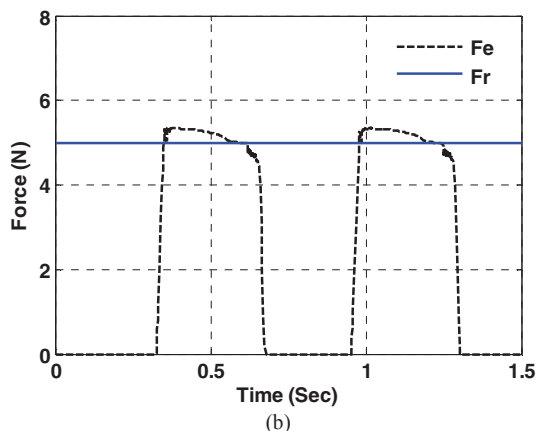
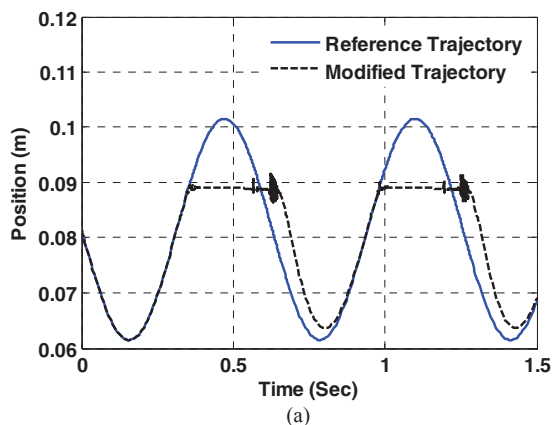


Fig. 14. Comparison of (a) reference and modified trajectories and (b) references and environment forces, when the impedance gains are adjusted by Fuzzy logic controller.

REFERENCES

- [1] J. S. Pap, W.L. Xu, and J. Bronlund, "A robotic human masticatory system –kinematics simulations," *Int J Intell Syst Tech Appl*, vol. 1, pp. 3-17, 2005.
- [2] W. Xu, J. E. Bronlund, "Mastication robots: biological inspiration to implementation," Springer-Verlag Berlin Heidelberg Press, 2010.
- [3] H. J. Smit a, E. K. Kemsley, H. S. Tapp, J. K. Henry, "Does prolonged chewing reduce food intake?," *Fletcherism revisited, Appetite*, vol. 57, pp. 295–298, 2011.
- [4] E. K. Kemsley, M. Defenez, J.C. Sprunt, A.C. Smith, "Electromyographic responses to prescribed mastication," *Journal of Electromyography and Kinesiology*, vol. 13, pp. 197-207, 2003.
- [5] Y. Ioannides, J. Seers , M. Defenez, C. Raithatha, M. S. Howarth, A. Smith, E. K. Kemsleys, "Electromyography of the masticatory muscles can detect variation in the mechanical and sensory properties of apples," *Food Qual Pref*, vol. 20, pp. 203-215, 2009.
- [6] W.E. Brown, "Method to investigate differences in chewing behaviour in humans: I. Use of electromyography in measuring chewing," *J Text Stud*, vol. 25, pp. 1-16, 1994.
- [7] F.R. Jack, J.R. Piggott, A. Paterson, "Relationships between electromyography, sensory and instrumental measures of cheddar cheese texture," *J Food Sci*, vol. 58, pp. 1313-1317, 1993.
- [8] W.E. Brown, K.R. Langley, L. Mioche, S. Marie, S. Gerault, D. Braxton, "Individuality of understanding and assessment of sensory attributes of foods, in particular, tenderness of meat," *Food Qual Pref*, vol. 7, pp. 205-216, 1996.
- [9] D. Braxton, C. Dauchel, W.E. Brown, "Association between chewing efficiency and mastication patterns for meat, and influence on tenderness perception," *Food Qual Pref*, vol. 7, pp. 217-223, 1996.
- [10] W.E. Brown, D. Braxton, "Dynamics of food breakdown during eating in relation to perceptions of texture and preference: a study on biscuits," *Food Qual Pref*, vol. 11, pp. 259-267, 2000.
- [11] N. Hogan, "Impedance control an approach to manipulation: part i-theory, part ii-implementation, part iii-applications," *Journal of Dynamic Systems, Measurement and Control*, 1985.
- [12] H. Kazerooni, "Robust, non-linear impedance control for robot manipulators," *Book Robust, non-linear impedance control for robot manipulators' (IEEE, 1987, edn.)*, pp. 741-750.
- [13] H. Seraji, and R. Colbaugh, "Force tracking in impedance control", *The International journal of robotics research*, 16, (1), pp. 97-117, 1997.
- [14] S. Jung, , T.C. Hsia and R.G Bonitz, "Force tracking impedance control of robot manipulators under unknown environment," *Control Systems Technology, IEEE Transactions on*, 12, (3), pp. 474-483, 2004.
- [15] S. Kizir, , and Z. BİNGÜL, "Fuzzy impedance and force control of a Stewart platform," *Turkish Journal of Electrical Engineering & Computer Sciences*, 22, (4), pp. 924-939, 2014.
- [16] Y. Li, S. S. Ge, "Force tracking control for motion synchronization in human-robot collaboration," *Robotica*, pp. 1-22, 2014,
- [17] R. Z. Stanisic, , and Á. V. Fernández, "Adjusting the parameters of the mechanical impedance for velocity, impact and force control," *Robotica*, 30, (04), pp. 583-597, 2012.
- [18] J. D. Torrance, "kinematics, motion control and force estimation of a chewing robot of 6rss parallel mechanism," *Ph.D thesis, Massy University, Palmerston North, New Zealand*, 2011.
- [19] A. Rezaee, H. Kalani, A. Akbarzadeh, "General Solution for the Dynamic Modeling of Stewart-Gough Platform Based on Principle of Virtual Work," *Nonlinear dynamics*, submitted.